Applied Catalysis B: Environmental 129 (2013) 98–105

Contents lists available at SciVerse ScienceDirect

Applied Catalysis B: Environmental

journal homepage: www.elsevier.com/locate/apcatb

Total oxidation of naphthalene using palladium nanoparticles supported on BETA, ZSM-5, SAPO-5 and alumina powders

Francisco J. Varela-Gandía[a], Ángel Berenguer-Murcia[a], Dolores Lozano-Castelló[a], Diego Cazorla-Amorós[a,*], David R. Sellick[b], Stuart H. Taylor[b,**]

[a] Materials Institute and Departamento de Química Inorgánica, Universidad de Alicante, Ap. 99, E-03080, Alicante, Spain
[b] Cardiff Catalysis Institute, School of Chemistry, Cardiff University, Main Building, Park Place, Cardiff CF10 3AT, UK

ARTICLE INFO

Article history:
Received 13 June 2012
Received in revised form 28 August 2012
Accepted 30 August 2012
Available online 10 September 2012

Keywords:
Catalytic oxidation
Zeolite BETA
ZSM-5
Pd nanoparticles
Naphthalene

ABSTRACT

A range of catalysts based on Pd nanoparticles supported on inorganic supports such as BETA and ZSM-5 zeolites, a silicoaluminophosphate molecular sieve (SAPO-5) and γ-alumina as a standard support have been tested for the total oxidation of naphthalene (100 ppm, total flow 50 ml/min) showing a conversion to carbon dioxide of 100% between 165 and 180 °C for all the analysed catalysts. From the combined use of zeolites with PVP polymer protected Pd based nanoparticles, enhanced properties have been found for the total abatement of naphthalene in contrast with other kinds of catalysts. A Pd/BETA catalyst has been demonstrated to have excellent activity, with a high degree of stability, as shown by time on line experiments maintaining 100% conversion to CO_2 during the 48 h tested.

1. Introduction

Polycyclic aromatic hydrocarbons (PAHs) are a family of volatile organic compounds (VOCs) produced mainly during combustion processes of organic matter [1,2]. PAH emissions originate from a great variety of sources, such as incomplete fuel combustion, diesel or gasoline, internal combustion engines, asphalt transformation plants or coal and wood powered plants [3,4]. According to the Environmental Protection Agency (EPA), a list containing 16 PAHs has been established as major pollutants whose emission must be controlled [5]. PAH compounds are mainly formed by several aromatic rings such as naphthalene (two-ring PAH), phenanthrene (three-ring PAH), pyrene or chrysene (four-ring PAH) or benzo[ghi]perylene (five-ring PAH). PAH composition differs depending on the emission source, and for example, PAHs found in diesel emissions mainly consist of two to five aromatic rings, and include naphthalene, phenanthrene, pyrene and fluoranthene [6,7]. The main reason to reduce PAH emissions is that they have now been identified as a serious environmental and health risk, due to their carcinogenic and/or mutagenic properties [8,9]. Naphthalene is the simplest and least toxic of the PAHs and it is thus used as a model compound for this group of pollutants.

The development of technologies to reduce atmospheric pollution has increased in recent years. Methods such as biodegradation, high-energy electron beam irradiation, ozonisation, adsorption, thermal incineration or catalytic oxidation have been employed to reduce the level of PAHs [2,10–15]. Despite the numerous options, catalytic oxidation to produce carbon dioxide and water is the most promising technology due to its lower operating temperature and/or higher selectivity to CO_2 [4,16].

Several studies have been performed to investigate the catalytic combustion of PAHs. Zhang et al. [6] have utilised noble metal catalysts supported on γ-alumina, indicating that precious metal catalyst such as Pd or Pt, were the most active in oxidising naphthalene. Garcia et al. [16] studied the total oxidation of VOCs, such as propane, benzene and naphthalene, with catalysts based on vanadium oxide, palladium oxide and mix Pd/V-supported on titania. Whilst for the case of aliphatic and one-ring aromatic compounds, $Pd/V/TiO_2$ was very promising, but Pd/TiO_2 was the most active for the total oxidation of naphthalene. On the other hand, a study of naphthalene combustion over a wide range of metal oxide catalysts, based on Co, Mn, Cu, Fe, Ce and Ti, have been carried out, establishing that nanocrystalline ceria was the most efficient catalyst for naphthalene removal [17]. In reference to zeolites, Neyestanaki et al. [18] have prepared metal exchanged zeolites for the removal of naphthalene in gas mixtures, simulating the emission from combustion biofuels by catalytic oxidation. In

* Corresponding author. Tel.: +34 965903946; fax: +34 965903454.
** Corresponding author.
E-mail addresses: cazorla@ua.es (D. Cazorla-Amorós), taylorsh@cf.ac.uk (S.H. Taylor).

0926-3373/$ – see front matter © 2012 Elsevier B.V. All rights reserved.
http://dx.doi.org/10.1016/j.apcatb.2012.08.041

more recent developments, mesoporous cerium oxides have also been prepared by nanocasting and they demonstrate appreciable activity for the total oxidation of naphthalene [4].

Despite all these previous studies, PVP polymer protected metal nanoparticles supported on inorganic oxides supports such as alumina or zeolites have not been studied yet for this reaction. During the last ten years, significant efforts have been dedicated to the preparation of nanoparticles. Their preparation, structure, characterisation and applications are issues of great current interest [19], with particular attention paid to the importance of their size and structure. Focusing on Pd nanoparticles, Teranishi and Miyake [20] dealt with the fundamental aspects of monometallic palladium nanoparticles, their synthesis and structural control, and the system has played an important role as a catalyst in numerous organic reactions. Within this field, unsupported Pd based nanoparticles have been used successfully in our group in the semihydrogenation of phenylacetylene [21] or supported on carbon [22] or inorganic materials [23]. Recently, Pd nanoparticles supported on γ-alumina have been successfully used in the PrO_x reaction [24], indicating the benefits of using PVP polymer protected Pd nanoparticles instead of Pd catalysts prepared by classical methods such as impregnation with a Pd compound and further reduction in hydrogen atmosphere.

Against this background, we have studied the use of powder catalysts based on Pd nanoparticles supported on two different zeolites (BETA and ZSM-5), a molecular sieve SAPO-5, and a more conventional γ-alumina support for the total oxidation of naphthalene. Special attention has been paid to the recyclability and stability of the catalyst over extended time-on-stream experiments. Catalysts have been characterised before and after use and this is important for assessing catalyst lifetime and stability.

2. Experimental

2.1. Catalyst preparation

Four supported catalysts were prepared by deposition of palladium nanoparticles onto selected inorganic supports. Pd nanoparticles protected by polyvinylpirrolidone (PVP) were synthesised using the reduction-by-solvent method previously described [24]. Four inorganic supports were used:

(1) The powder γ-alumina support was provided from Alfa Aesar 99.97% (Ref. 039812).
(2) Two zeolites, BETA and ZSM-5. The procedure followed for the synthesis of these materials has been described elsewhere [25].
(3) A silicoaluminophosphate molecular sieve SAPO-5 was prepared following the method described by Campelo et al. [26].

The catalysts used in this work were prepared by the impregnation method, as reported previously by our group [22–24]. In a typical procedure, 3 g of support was mixed with the appropriate amount of the purified colloidal suspension to yield 1 wt% of metallic loading. The solution was stirred for two days at room temperature in order to ensure a similar load and dispersion for the different catalysts, and transferred to an oven, where it was left at 60 °C in order to evaporate the solvent. The catalysts were then washed several times with a cold mixture of H_2O/EtOH (50:50, v/v), and left to dry overnight at 60 °C.

2.2. Catalyst characterisation

ZSM-5 and BETA zeolites and SAPO-5 silicoaluminophosphate molecular sieve were characterised by XRD, using a 2002 Seifert powder diffractometer. The scanning rate was 2°/min and Cu Kα radiation was used.

TEM images of the catalysts were recorded in a JEOL (JEM-2010) electron microscope equipped with an EDS analyser (OXFORD, model INCA Energy TEM 100) operating at 200 kV with a space resolution of 0.24 nm. For the analysis, a small amount of the catalyst was suspended in a few drops of methanol, and sonicated for a few minutes. A drop of this suspension was then deposited onto a 300 mesh Lacey copper grid and left to dry at room temperature. The diameter of the nanoparticles and the dispersion of the metal over the catalyst were determined as described previously [24].

The textural characterisation of the catalysts was carried out by means of the adsorption of N_2 at −196 °C and CO_2 at 0 °C (Autosorb 6, Quantachrome). Prior to the adsorption measurements, the catalysts were outgassed under vacuum (10^{-2} mbar) at 250 °C for 4 h to remove any adsorbed impurities. Surface area was calculated from nitrogen adsorption isotherms using the BET equation (S_{BET}). Total micropore volume (V_{DR} (N_2)) and narrow micropore volume (V_{DR} (CO_2)) were calculated by applying the Dubinin–Radushkevich (DR) equation to the N_2 adsorption data at −196 °C and the CO_2 adsorption data at 0 °C, respectively [27].

The metal loading of the catalysts was analysed by inductively coupled plasma-optical emission spectroscopy (ICP-OES), in a PerkinElmer Optima 4300 system. The extraction of the metal was made by an oxidative treatment of the samples with aqua regia, followed by filtration of the remaining solid using a nylon membrane filter (average pore diameter of 400 nm) and dilution of the resulting metal solution using a volumetric flask.

XPS measurements were made on an Omicron ESCA+ photoelectron spectrometer using a non-monochromatised Mg Kα X-ray source ($h\nu$ = 1253.6 eV). An analyser pass energy of 50 eV was used for survey scans and 20 eV for detailed scans. Binding energies are referenced to the C1s peak assumed to have a binding energy of 284.5 eV.

Thermogravimetric analysis (TGA) experiments were performed in a Thermogravimetric Analyzer (TA Instruments, model SDT 2960). In these experiments, approximately 10 mg of the catalyst (fresh and used) were treated. The catalyst was heated up to 900 °C (heating rate of 10 °C/min) and equilibrated for 1 h, under a constant flow rate of 100 ml/min air.

2.3. Catalyst testing

Catalytic activity tests for naphthalene oxidation were carried out in a fixed bed reactor (diameter: 1.6 cm). The feed stream consisted, in all cases, of 100 vppm naphthalene in a mixture of 20%O_2 and 80%He. The total flow (F) was set to 50 ml/min and a catalyst powder weight (m) of 200 mg (F/m = 15 L/g h). Analysis of reactants and reaction products was performed by on-line gas chromatography using thermal conductivity and flame ionisation detectors. Catalytic activity was measured over the temperature range 100–200 °C in incremental steps (100, 125, 150, 165, 180, 195 and 200 °C), and temperatures were measured by a thermocouple placed in the catalyst bed connected to a PID controller. Data were collected at each temperature after a stabilisation time of 20 min. Three analyses were made at each temperature to ensure that steady state data were collected. Oxidation activity is expressed as a yield of carbon dioxide. The turnover frequency (TOF in s^{-1}), defined as moles of CO_2 generated per mole of surface metal per second, was determined taking into account the amount of naphthalene converted to CO_2 in the gas stream used in the experiments. The mole of surface metal was calculated using the metal concentration obtained by the ICP technique and the metal dispersion calculated by TEM. Activation energies were calculated at low temperatures for conversions lower than 20%, applying the Arrhenius equation. Furthermore, time-on-line experiments for long-term

Table 1
Porous texture characterisation of the supports and prepared catalyst.

Sample	S_{BET} (m^2/g)	$V_{DR}(N_2)$ (ml/g)	$V_{DR}(CO_2)$ (ml/g)
BETA	570	0.25	0.21
Pd/BETA	510	0.22	0.18
ZSM-5	290	0.14	0.11
Pd/ZSM-5	270	0.12	0.11
SAPO-5	210	0.10	0.18
Pd/SAPO-5	105	0.07	0.13
γ-Alumina	70	0.03	0.03
Pd/γ-alumina	50	0.02	0.02

use of these catalysts were performed with the aim to probe possible deactivation. For this purpose, the catalysts were tested using reaction conditions the same as described above but at a higher temperature of 250 °C for 48 h. This approach of an accelerated ageing test is common for evaluating catalysts for potential application of VOC abatement.

3. Results and discussion

3.1. Catalysts characterisation

Firstly, the as synthesised materials, BETA, ZSM-5 and SAPO-5 were characterised by XRD, confirming the typical structure for each material. Moreover, after the impregnation method, the catalysts were analysed by XRD and no change was observed in the prepared catalysts (results not shown), indicating that the process of introducing the Pd nanoparticles did not compromise the structure of the supports.

Nitrogen adsorption was performed to investigate the porous texture of the as prepared materials, and any changes that may have occurred due to nanoparticle deposition during catalyst preparation. From the N_2 isotherms (results not shown), it is possible to confirm that BETA, ZSM-5 and SAPO-5 exhibit a Type I isotherm, which according to IUPAC classification [28] is typical of microporous solids. γ-Al_2O_3 shows a Type II isotherm [28] typical of macroporous materials. After preparing the catalyst, the adsorption/desorption isotherms of the catalysts did not exhibit any noticeable change in the isotherm shape, indicating that although the adsorbed amounts decreased for all the prepared catalysts, with respect to the original support, none of the samples showed evidence for loss of porosity or creation of new porosity. Table 1 summarizes the surface areas (S_{BET}), the total micropore volume ($V_{DR}(N_2)$) and narrow micropore volume ($V_{DR}(CO_2)$). Analysing the results in depth, it can be established that the catalyst preparation method has affected the porosity of the supports. According to the N_2 adsorption isotherms the amount of N_2 adsorbed on the catalysts diminished in all cases with respect to the supports alone (see S_{BET} and $V_{DR}(N_2)$ in Table 1). Pd/BETA and Pd/ZSM-5 showed reduced adsorption properties to a minor extent. Nevertheless, the Pd/SAPO-5 catalyst showed a considerably reduced apparent surface area while still being a microporous material as mentioned previously. The Pd/γ-Al_2O_3catalyst had reduced specific BET surface area, although it is a macroporous material. Therefore, it can be ascertained that the catalyst preparation method affects the porous texture, especially the microporosity. This occurred to a minor degree for BETA and ZSM-5 supports, but to a more significant extent for the SAPO-5 support.

Fig. 1 shows the TEM images of the Pd colloid together with the four catalysts prepared for this work. As can be extracted from the TEM micrographs of the colloid, the synthesised colloid shows very low polidispersity for the size of the particles. From the different images of the different catalysts prepared for this work, the deposition of polymer-protected nanoparticles results in a noticeable change in Pd particle size, which agrees with our previous studies [22–24]. Therefore, TEM micrographs show an effect on the size of the particles during catalyst preparation, as the mean particle size slightly increases from the starting colloid to the final catalyst. Table 2 shows the diameter of the prepared particles (d) before and after deposition on the supports and the dispersion (D) of the nanoparticles, calculated according to a procedure described in detail elsewhere, assuming a spherical particle shape [29]. Metal

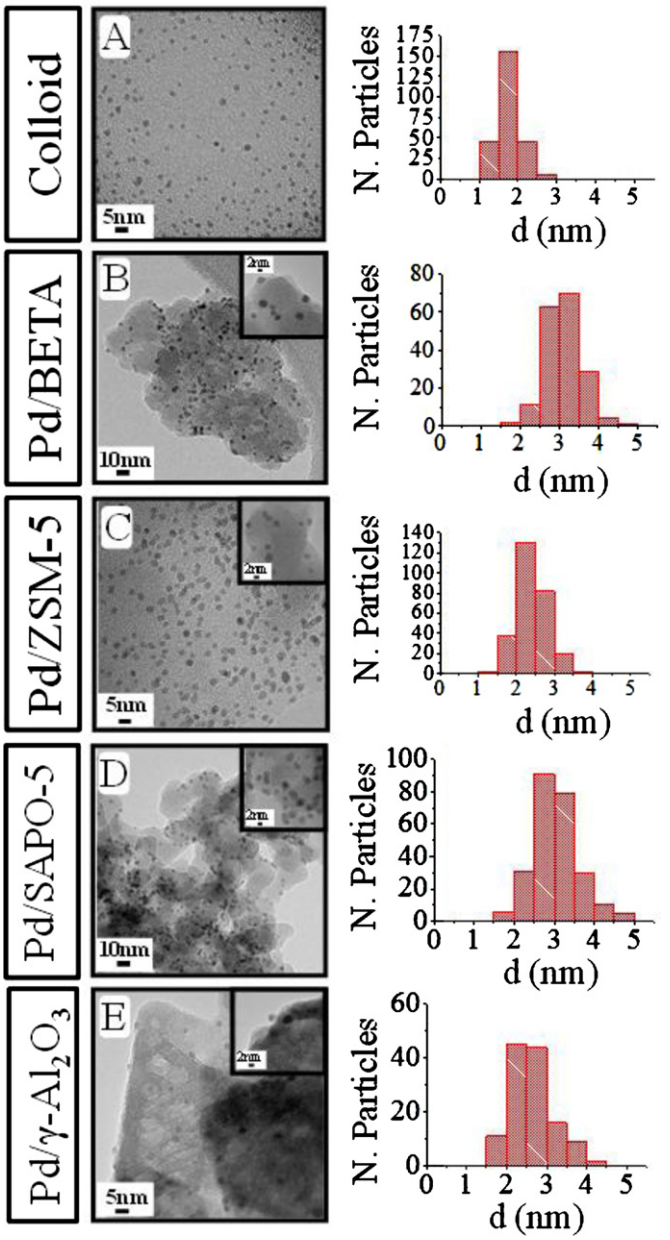

Fig. 1. TEM images and particle size distribution of: (A) colloid; (B) Pd/BETA; (C) Pd/ZSM-5; (D) Pd/SAPO-5; (E) Pd/γ-Al_2O_3.

Table 2
Nanoparticles sizes obtained from TEM data and metal loading of the different catalysts.

Sample	d TEM (nm)	D TEM (%)	Metal loading (wt%)
Pd colloid	1.7 ± 0.3	–	–
Pd/BETA	3.1 ± 0.5	29	0.54
Pd/ZSM-5	2.4 ± 0.4	38	0.74
Pd/SAPO-5	3.1 ± 0.6	29	0.74
Pd/γ-Al_2O_3	2.6 ± 0.2	35	0.38

Table 3
Temperature required for naphthalene total oxidation for the different catalysts for the four oxidation cycles tested and coke deposition after 4 cycles.

Sample	T (°C) for total conversion to CO_2				Coke deposited (%) after 4 cycles
	Cycle 1	Cycle 2	Cycle 3	Cycle 4	
Pd/BETA	180	180	165	165	3.3
Pd/ZSM-5	165	165	165	165	0.8
Pd/SAPO-5	195	180	180	180	1.2
Pd/γ-Al_2O_3	180	180	180	195	0

loading (wt%) calculated by ICP analyses are included in Table 2. The Pd loading of the catalysts varies by nearly a factor of 2. The reason for such a difference is not straightforward and must be related to both the surface roughness of the supports and to the interaction among the polymer-protected Pd nanoparticles and the support.

3.2. Catalytic performance for naphthalene oxidation

The catalytic activity for naphthalene oxidation was measured for the four catalysts. Four cycles of increasing and then reducing reaction temperature were performed with each catalyst in order to ensure the stability of the sample. The main reaction product observed for naphthalene oxidation was CO_2. Nevertheless, by-products such as phthalic anhydride, naphthanol, ketone, benzoic acid and 1,2-dibenzoic acid were also detected in very low concentrations under certain reaction conditions when conversion was relatively low. These compounds were trapped in acetone using an acetone/ice cold trap at the exit of the reaction system and then analysed by GC–MS. The reaction temperature was fixed between 100 and 200 °C, depending on the catalyst, and products collected for 2 h. In addition, it is worth noting that CO was not detected as a reaction product in any of the experiments performed.

Table 3 shows the temperature required for total naphthalene oxidation to CO_2 for each catalyst over the four temperature cycles. Excellent catalytic performance has been observed for each of the four catalysts. Analysing these results thoroughly, Pd/BETA and Pd/ZSM-5, show a lower temperature for total naphthalene conversion, whilst Pd/SAPO-5 and Pd/γ-Al_2O_3 are able to reach full naphthalene conversion at slightly higher temperatures. For comparative purposes, the activity of the support for the most active catalyst was measured. BETA zeolite was only active at temperatures above 300 °C, reaching a conversion to CO_2 of 64% at 350 °C. Hence the zeolite support without the Pd nanoparticles was totally inactive over the temperature range where the Pd-based catalyst showed total naphthalene conversion.

The Arrhenius plots for the first reaction cycle for all catalysts were made (results not shown). The linearity of these plots at low temperatures where low conversions (<20%) are obtained, indicated that the reaction is in the chemical kinetically controlled regime. Table 4 shows the calculated apparent activation energies (E_a) and the values obtained indicated that there were no diffusional limitations for the reaction tested. Table 4 includes the turnover frequency (TOF) for the four catalysts during the first catalytic reaction cycle. For comparison purposes, the TOF for a 0.5%Pt/SiO_2 catalyst tested previously for the same reaction, under very similar conditions [30], has been included. Interestingly, despite using the same Pd-PVP nanoparticles in all the catalysts tested, the TOF and E_a were different depending on the support, demonstrating E_a values for the Pd/γ-Al_2O_3 which are four times greater than that found for the Pd/BETA catalyst. Therefore, close inspection of the influence of the support is necessary to explain the different activity data for the four catalysts tested. Comparing our results for the different catalysts tested with one prepared by classical impregnation, Pt/SiO_2 [30], it is possible to observe that the Pd-PVP nanoparticle based catalysts have much greater TOF than a standard silica supported Pt-based catalyst, indicating the potential of these kind of nanoparticles which can be easily tuned during the preparation method to adapt their properties to the desired reaction. Hence, with the aim of explaining the different behaviour of the catalysts special attention needs to be paid to the important influence of the support on the catalytic activity. In this respect, supports which strong surface acidity may favour the naphthalene oxidation reaction when used in conjunction with Pd-PVP nanoparticles.

Table 4
Turnover frequency (TOF) at 125 °C and apparent activation energy for the four catalysts at first reaction cycle.

Sample	Data from first cycle	
	TOF (s^{-1}) (T = 125 °C)	E_a (kJ/mol)
Pd/BETA	0.075	46
Pd/ZSM-5	0.056	55
Pd/SAPO-5	0.010	126
Pd/γ-Al_2O_3	0.019	166
0.5%Pt/SiO_2 [30]	0.0007	–

The higher activity of the ZSM-5 and BETA catalysts may be associated with the porous texture of the catalyst. Thus, Pd/BETA and Pd/ZSM-5 both present a significant surface area that may have an influence on the activity during the total oxidation, and therefore, there may be a relationship between the apparent surface area of the catalyst and its capacity to oxidize naphthalene. Moreover, the pore size distribution and channel interconnectivity may also have an important contribution, in agreement with Puertolas et al. [4], who studied the use of different mesoporous cerium oxides prepared through nanocasting method for the total oxidation of naphthalene, mentioning that wider pore size distributions and pore interconnectivity could facilitate the total oxidation of naphthalene. In this sense, the zeolite supports BETA and ZSM-5, which have a three-dimensional pore size distribution, present a high interconnectivity, in contrast to SAPO-5 acting as a support which presents a one-dimensional porosity with a larger pore size than zeolites BETA or ZSM-5. Considering the pore size of the selected supports, it is clear that the Pd nanoparticles will be deposited solely on the outer surface of the microporous zeolites and silicoaluminophosphate, whereas in the case of the macroporous support (γ-Al_2O_3) the nanoparticles will be deposited both in the inner and outer surface. The location of the particles indicates that while the inner surface area of the selected supports does not play a significant role in the oxidation of naphthalene as such, it clearly influences the outcome of the catalytic reaction. The supports with a larger surface area, in this respect, may adsorb larger amounts of naphthalene in their porous structure, thus acting as "naphthalene reservoirs" which feed the Pd particles where the catalytic oxidation takes place, which could help to explain our results.

It is well known that BETA zeolite has a relatively high external surface area resulting from its structure being the combination of two intergrown polymorphs. This high external surface area may result in increased accessibility for naphthalene molecules to reach the Pd nanoparticles of the catalyst, as well as a possible reservoir

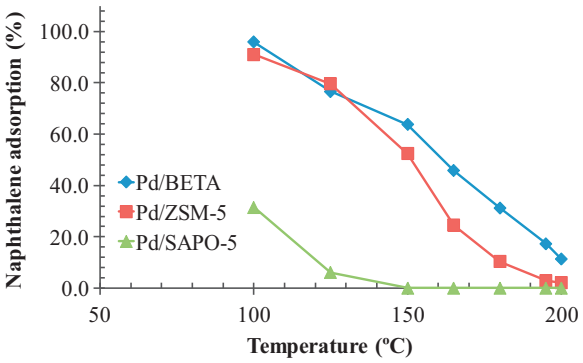

Fig. 2. Variation of the amount of naphthalene adsorbed as a function of temperature on the three catalysts.

for naphthalene molecules. As a consequence, total oxidation of naphthalene to CO_2 can be reached at lower temperatures. It is also possible that the adsorption of naphthalene onto the catalysts could be significant and could provide a reservoir for naphthalene. In order to verify this, the Pd/BETA, Pd/ZSM-5 and Pd/SAPO-5 catalysts were tested under the same conditions as the aforementioned oxidation experiments, but without O_2 in the reactant flow, in order to study the contribution of the catalyst towards naphthalene adsorption. The catalyst Pd/γ-Al_2O_3 was excluded from this experiment, because from the catalytic oxidation experiments it became evident that the Pd/γ-Al_2O_3 catalyst did not exhibit any significant naphthalene adsorption during the reaction time of about 1 h and at the lowest temperature used. That is, naphthalene in the gas stream leaving the reactor at this temperature contained 96 ppm of naphthalene, which corresponds to 96% of the initial concentration in the inlet stream. Fig. 2 shows the amount of naphthalene adsorbed by the different catalysts during a time similar to that used in the experiments in the presence of oxygen and over the temperature range studied. According to these results, the amount of adsorbed naphthalene in Pd/SAPO-5 is lower when compared with the zeolite based-catalysts. Furthermore, there is no appreciable naphthalene adsorption above 150 °C. On the contrary, Pd/BETA and Pd/ZSM-5 present a much larger adsorption capacity for naphthalene at higher temperatures. This adsorbed naphthalene may act as a "reservoir" to feed the catalysts in the initial stages of the reaction, thus increasing the efficiency of the catalyst. Considering this feature, Pd/BETA and Pd/ZSM-5 may permit naphthalene oxidation at lower temperatures than Pd/SAPO-5. Therefore, the three-dimensional pore structure and the high adsorption capacity seem to play an important role in the performance of the catalyst.

Although Pd/BETA was the most active catalyst after four cycles, another outstanding feature was the reduction of the temperature at which total conversion to CO_2 was achieved as the number of cycles was increased, whilst the temperature for total oxidation for Pd/ZSM-5 remains unchanged after four cycles. This could be explained by considering that in the case of the Pd/BETA catalyst there was coke deposition during the first cycle (evident by a change of colour from grey to black upon completion of the first catalytic cycle). As the catalyst was used coke deposition was reduced, producing naphthalene oxidation to CO_2 at lower temperatures. In this sense, our results reveal that the amount of coke deposited after 4 cycles (see Table 3) does not affect the catalytic activity of the studied systems in terms of deactivation. It must be noted that the amounts of coke deposited on the different catalysts (which go from 3.3% to 0.8%) were not considered significant towards the determination of catalytic naphthalene conversion to CO_2 (this becomes clear upon observing the error bars when determining said activity) or to affect the C balance to any significant degree.

Another parameter that can have an influence on the catalytic activity is the stability of the samples. Fig. 3 shows the variation of the catalytic activity (expressed as conversion to CO_2) for naphthalene oxidation, as a function of the reaction temperature. According to these results, the catalytic activity for Pd/BETA, Pd/ZSM-5 and Pd/SAPO-5 remained unchanged after four cycles and maintained high naphthalene oxidation activity towards the formation of CO_2. In contrast, Pd/γ-Al_2O_3 showed an increase in the temperature for total oxidation after the completion of the four cycles and this can tentatively be attributed to the deactivation of the catalyst. With the aim to distinguish differences between deactivation of

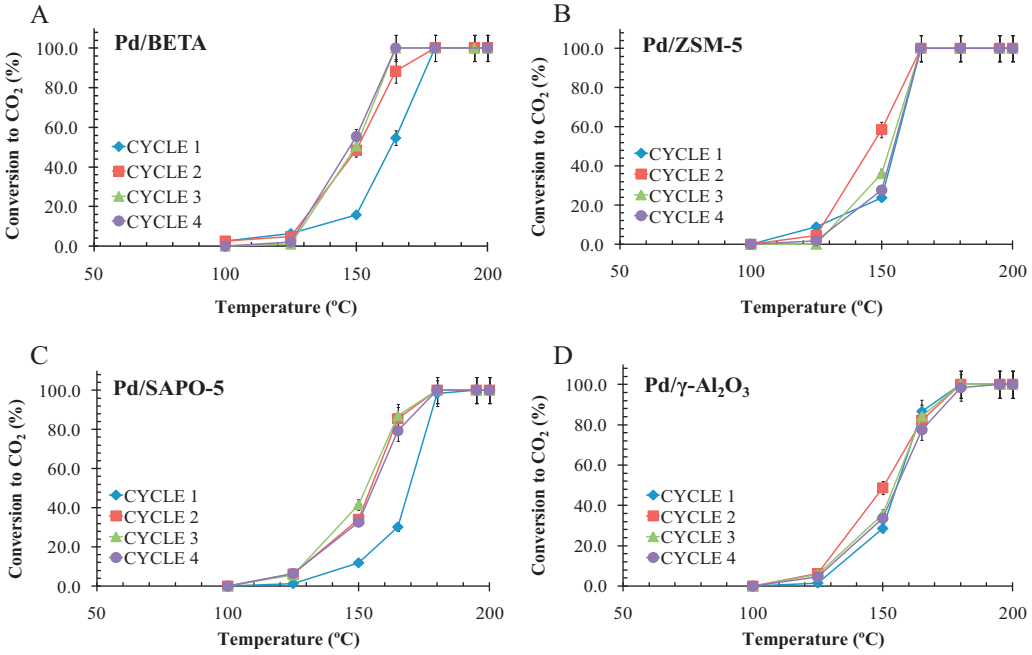

Fig. 3. Variation of the catalytic activity for naphthalene oxidation (expressed as yield to CO_2) as a function of reaction temperature over the four catalysts. (A) Pd/BETA; (B) Pd/ZSM-5; (C) Pd/SAPO-5; (D) Pd/γ-Al_2O_3.

Table 5
CO_2 conversion at 150 °C for the four catalysts and during the four cycles tested.

Sample	CO_2 conversion (%) (T = 150 °C)			
	Cycle 1	Cycle 2	Cycle 3	Cycle 4
Pd/BETA	16	49	51	56
Pd/ZSM-5	24	59	31	28
Pd/SAPO-5	12	34	42	33
Pd/γ-Al_2O_3	29	48	37	34

these three catalysts, it is necessary to analyse their behaviour at intermediate temperatures. Therefore, in order to probe potential deactivation, catalytic activity at 150 °C is summarised in Table 5. Despite appearing to be relatively stable after four temperature cycles, the yield of CO_2 during incomplete conversion at 150 °C can provide further information on which is the most suitable for naphthalene total oxidation. Consequently, focusing our attention on these values the Pd/BETA catalyst is not affected after four cycles, while Pd/ZSM-5 and Pd/SAPO-5 showed reduced overall conversion after four catalytic cycles, this decrease being more moderate for Pd/SAPO-5 and more pronounced for Pd/ZSM-5.

TEM analyses were performed on the used catalysts after reaction, with the aim to analyse any significant effect of the reaction conditions on the catalyst. Fig. 4 illustrates the TEM micrographs of the four used catalysts and the diameter of the Pd particles (d) and the dispersion of the catalysts (D) after the reaction cycles included in Table 6. From the TEM analysis it can be concluded that all the

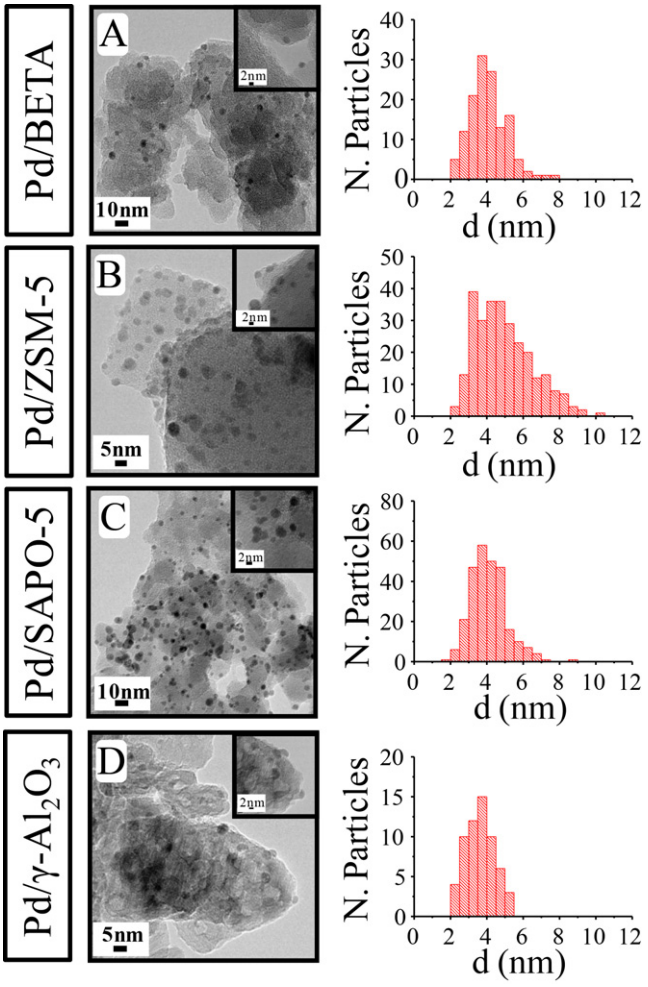

Fig. 4. TEM images and particle size distribution of catalysts used after four cycles of naphthalene oxidation: (A) Pd/BETA; (B) Pd/ZSM-5; (C) Pd/SAPO-5; (D) Pd/γ-Al_2O_3.

Table 6
Results of Pd nanoparticle analysis by TEM for catalysts after testing in naphthalene oxidation.

Sample	d TEM (nm)	D TEM (%)
Pd/BETA	4.1 ± 1.0	22
Pd/ZSM-5	5.0 ± 1.5	18
Pd/SAPO-5	4.1 ± 1.0	22
Pd/γ-Al_2O_3	3.6 ± 0.7	25

Table 7
XPS analysis of the four catalysts used, before and after use for naphthalene oxidation.

		BE Pd $3d_{5/2}$		Pd percentage (%)	
		Prepared	Tested	Prepared	Tested
Pd/BETA	Pd(0)	335.1	335.3	47	52
	Pd(II)	336.4	336.7	53	48
Pd/ZSM-5	Pd(0)	334.9	335.1	64	40
	Pd(II)	336.9	337	36	60
Pd/SAPO-5	Pd(0)	335.2	335.3	80	65
	Pd(II)	337.1	337.2	20	35
Pd/γ-Al_2O_3	Pd(0)	335.6	335.8	69	54
	Pd(II)	336.8	337.0	31	46

Pd nanoparticles in the catalysts have increased in size. Despite this increase in particle size, only the Pd/alumina catalyst has shown a significant increase in the temperature for total oxidation after four cycles. Therefore, the rest of the catalysts have demonstrated high stability for oxidation of naphthalene and the increase of Pd particle size has not had a major detrimental effect on activity.

XPS analyses were performed on the fresh and used catalysts. Table 7 shows the results corresponding to the atomic percentage of the different Pd species present on the catalyst surface and the binding energy of each of the species determined through curve fitting. The XPS binding energies revealed the presence of two peaks corresponding to the $3d_{3/2}$ and $3d_{5/2}$ transitions. In the case of prepared samples, the presence of Pd(II) on the surface of the Pd nanoparticles is attributed to the carbonyl function of the protecting polymer interacting with the metallic palladium, removing electron density from the surface, as has been established in our previous work [24] and by Somorjai and co-workers [31–33] for Pt nanoparticles capped with this kind of agent. In short, what appears in this case as Pd(II) in the XPS spectra, is attributed to the palladium atoms on the surface of the nanoparticle, which are electron deficient due to their interaction with the protecting polymer. Following on, the greater amount of Pd(II) present in the Pd/BETA with respect to the other catalysts could be due to a stronger interaction of Pd with PVP than for PVP with the support, which in turn may affect the catalytic activity. In contrast, Pd/ZSM-5, Pd/SAPO-5 and Pd/γ-Al_2O_3 catalysts have a stronger PVP-support interaction that produces a reduction in the electronic density withdrawn and therefore, the quantity of Pd(0) is higher. Once all the catalysts were tested, the amount of Pd(II) increased in all the catalysts except on the surface of the Pd/BETA catalyst, indicating that the Pd/nanoparticles were partially oxidised, producing Pd(II) species on the Pd nanoparticle surface. On the one hand it could be stated that the Pd nanoparticle is protected by the PVP due to a stronger interaction of Pd with PVP and this makes the Pd nanoparticle more resistant towards oxidation. On the other hand, the Pd/BETA catalyst increased the intensity of the Pd(0) signal. This phenomenon could be attributed to the Pd/BETA catalyst being more stable due to the aforementioned stronger interaction between the Pd nanoparticles and the protecting polymer. The importance of the protection can be better assessed upon analysing the conversion of naphthalene at 150 °C (see Table 5). Thus, despite having the lowest Pd(0)/Pd(II) ratio in

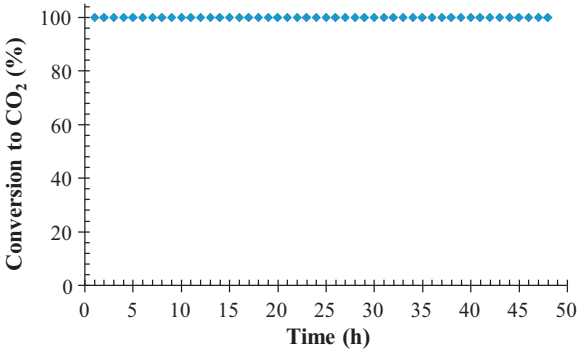

Fig. 5. Conversion of naphthalene to CO_2 as a function of time-on-line at 250 °C for the Pd/BETA catalyst.

the fresh catalyst (see Table 7), the PVP–Pd interaction explains the absence of deactivation of this catalyst as the sample is submitted to successive reaction cycles. On the contrary, the rest of the prepared catalysts, which have a higher initial Pd(0)/Pd(II) ratio, have a lower conversion at 150 °C (see Table 5) because the interaction between the Pd nanoparticles and the protecting polymer is less intense than the Pd/BETA catalysts, rendering them more susceptible to surface oxidation. Another possible reason that could be preventing Pd nanoparticle oxidation is associated with the coke deposition produced on the Pd/BETA catalyst. Apart from zeolite BETA acting as a cracking catalyst, the Pd(II) produced on the surface is being reduced due to this enhanced effect between the Pd nanoparticles and BETA zeolite that can promote the reduction of Pd(II) at the surface to Pd(0) and the oxidation of part of this deposited coke. Therefore, the Pd/BETA catalyst has different behaviour, making it more stable than the rest of the catalysts.

The Pd/BETA catalyst was identified as the most effective metal-supported catalyst for naphthalene total oxidation. Therefore, long-term use of this catalyst, in order to start to evaluate the catalyst life-time, was performed. Earlier studies indicated that activity was stable and the catalyst was able to produce total naphthalene conversion at low temperatures between 165 and 180 °C. An additional accelerated ageing stability study was conducted at 250 °C for 48 h, this elevated temperature was chosen in order to accelerate potential sintering of the active palladium nanoparticles. Fig. 5 shows the time-on-line data for the Pd/BETA catalyst. It was evident that the catalyst maintained 100% naphthalene conversion over the 48 h test period. The yield of CO_2 at the beginning of the experiment was 100% and it was not diminished after 48 h. As conversion was greater than 100% it is not possible to unequivocally state there was no catalyst deactivation and much longer reaction times and data collected at conversion below 100% would be required to more fully establish any catalyst deactivation. Although the Pd/BETA was the best catalyst, the time-on-line activity of Pd/ZSM-5 was also analysed in the same manner and it showed equally stable 100% conversion to CO_2 over the reaction time (results not shown).

With respect to naphthalene total oxidation, in the literature it is possible to find several research studies focused on using metal supported catalysts, prepared by conventional methods, or metal oxide catalysts for naphthalene oxidation. Neyestanaki et al. [18] have studied the use of ZSM-5 impregnated with different concentrations of Pd to remove the emission of pollutants from the combustion of biofuels. In this study, the catalysts were used for four consecutive cycles, with three different gas mixtures varying the composition of different polluting gases including always 50 ppm of naphthalene. In terms of naphthalene conversion, it can be seen that our catalyst based on Pd nanoparticles exhibits a naphthalene total conversion between 165 and 180 °C. Meanwhile, the catalyst prepared by the impregnation method from the aforementioned work needed a temperature of 400 °C to achieve total conversion for the Na-form of the ZSM-5 zeolite. On the other hand, the H-form of the ZSM-5 reduced the temperature for total conversion to 200 °C, however, catalyst deactivation was observed. Also using a Pd-based catalyst, Zhang et al. [6] studied the oxidative decomposition of naphthalene (100 ppm) by a supported Pd/γ-Al_2O_3 catalyst, and it demonstrated 90% conversion to CO_2 at 285 °C, but total conversion was not reached until approximately 400 °C. Furthermore, Garcia et al. [16] studied the total oxidation of naphthalene (100 ppm) with a Pd/TiO_2 catalyst, which produced a total conversion to CO_2 at approximately 270 °C, which was a lower temperature than Zhang et al. [6]. In addition, it was reported that naphthalene physisorption on the catalyst had an important role in the catalysed reaction with Pd/TiO_2. Therefore, our catalysts supported on zeolites based on PVP stabilised Pd nanoparticles appear to be more stable than those prepared by conventional impregnation methods, and the total conversion to CO_2 is achieved at lower temperatures.

Comparing our results with those obtained with other kinds of catalysts, it is possible to observe that the total oxidation of naphthalene is reached at lower temperatures with our zeolite supported catalysts. In the case of metal oxide catalysts [17] such as CeO_2 or mixed oxides (CuZnO) full conversion is reached at temperatures between 250 °C and 270 °C, respectively. Whilst for the case of metals supported on different oxides such as Pt/SiO_2 [30] the optimum temperature for naphthalene oxidation was 250 °C. Shie et al. [34] indicated that Pt/γ-alumina decreased the reaction temperature for 95% naphthalene total oxidation to 207 °C. On the other hand, Pt supported on mesoporous materials have also been used. Park et al. [35] have prepared Pt/MCM41 and Pt/SM41 (SM: molecular sieve) and used them as catalysts for the total oxidation of naphthalene in dry and wet conditions, establishing the reaction temperature for total conversion to CO_2 at 300 °C. To conclude, the combination of Pd-based nanoparticles with zeolites, BETA and ZSM-5, permits the total oxidation of naphthalene at substantially lower temperatures (165 °C) than many catalysts reported in the literature. However, these promising catalysts should be tested using wet feed stream to analyse the effect of water in naphthalene oxidation.

4. Conclusions

Zeolites BETA and ZSM-5, silicoaluminophosphate molecular sieve, SAPO-5 and γ-alumina impregnated with Pd nanoparticles have been used as catalysts for the total oxidation of naphthalene. All the catalysts produced high activity for naphthalene conversion to CO_2, with total conversion taking place between 165 and 180 °C. Pd/BETA was the most active catalyst. Furthermore, all the catalysts have high stability because their properties remain largely unchanged after testing for several oxidation cycles. Time-on-line experiments have been used to test the stability of the catalysts. The Pd/ZSM-5 and Pd/BETA samples were stable after accelerated ageing time-on-line for 48 at 250 °C. Therefore, the use of Pd-based nanoparticles supported on zeolites (BETA or ZSM-5) could be potential options for the abatement of PAHs by catalytic oxidation.

Acknowledgments

The authors would like to thank the Spanish Ministerio de Ciencia e Innovación and PLAN E funds (Project CTQ2009-10813/PPQ) and Generalitat Valenciana and FEDER (PROMETEO/2009/047) for financial support.

F.J. Varela-Gandía thanks the University of Alicante for the PhD studentship. Á. Berenguer-Murcia thanks the Spanish Ministry for

Science and Innovation for a Ramon y Cajal fellowship (RyC 2009-03913).

References

[1] B. Solsona, T. Garcia, R. Murillo, A.M. Mastral, E. NtainjuaNdifor, C.E. Hetrick, M.D. Amiridis, S.H. Taylor, Topics in Catalysis 52 (2009) 492–500.
[2] M.H. Yuan, C.Y. Chang, J.L. Shie, C.C. Chang, J.H. Chen, W.T. Tsai, Journal of Hazardous Materials 175 (2010) 809–815.
[3] F. Diehl, J. Barbier Jr., D. Duprez, I. Guibard, G. Mabilon, Applied Catalysis B 95 (2010) 217–227.
[4] B. Puertolas, B. Solsona, S. Agouram, R. Murillo, A.M. Mastral, A. Aranda, S.H. Taylor, T. Garcia, Applied Catalysis B 93 (2010) 395–405.
[5] A.M. Mastral, M.S. Callen, Environmental Science and Technology 34 (2000) 3051–3057.
[6] X. Zhang, S. Shen, L.E. Yu, S. Kawi, K. Hidajat, K.Y. Simon Ng, Applied Catalysis A 250 (2003) 341–352.
[7] J.I. Park, J.K. Lee, J. Miyawaki, S.H. Yoon, I. Mochida, Journal of Industrial and Engineering Chemistry 17 (2011) 271–276.
[8] E.N. Ndifor, T. Garcia, S.H. Taylor, Catalysis Letters 110 (2006) 125–128.
[9] S.C. Kim, S.W. Nahm, W.G. Shim, J.W. Lee, H. Moon, Journal of Hazardous Materials 141 (2007) 305–314.
[10] E.N. Ndifor, S.H. Taylor, Topics in Catalysis 52 (2009) 528–541.
[11] C.C. Chang, C.Y. Chiu, C.Y. Chang, C.F. Chang, Y.H. Chen, D.R. Ji, Y.H. Yu, P.C. Chiang, Journal of Hazardous Materials 161 (2009) 287–293.
[12] L. Yu, X. Li, X. Tu, Y. Wang, S. Lu, J. Yan, Journal of Physical Chemistry A 114 (2010) 360–368.
[13] M.H. Yuan, Y.Y. Lin, C.Y. Chang, C.C. Chang, J.L. Shie, C.H. Wu, IEEE Transactions On Plasma Science 39 (2011) 1092–1098.
[14] S.C. Marie-Rose, T. Belin, J. Mijoin, E. Fiani, M. Taralunga, F. Nicol, X. Chaucherie, P. Magnoux, Applied Catalysis B 90 (2009) 489–496.
[15] A. Bampenrat, V. Meeyoo, B. Kitiyanan, P. Rangsunvigit, T. Rirksomboon, Catalysis Communications 9 (2008) 2349–2352.
[16] T. Garcia, B. Solsona, D. Cazorla-Amorós, Á. Linares-Solano, S.H. Taylor, Applied Catalysis B 62 (2006) 66–76.
[17] T. Garcia, B. Solsona, S.H. Taylor, Applied Catalysis B 66 (2006) 92–99.
[18] A.K. Neyestanaki, L.E. Lindfors, T. Ollonqvist, J. Väyrynen, Applied Catalysis A 196 (2000) 233–246.
[19] M. Moreno-Mañas, R. Pleixats, Accounts of Chemical Research 36 (2003) 638–643.
[20] T. Teranishi, M. Miyake, Chemistry of Materials 10 (1998) 594–600.
[21] S. Domínguez-Domínguez, Á. Berenguer-Murcia, D. Cazorla-Amorós, Á. Linares-Solano, Journal of Catalysis 243 (2006) 74–81.
[22] S. Domínguez-Domínguez, Á. Berenguer-Murcia, B.K. Pradhan, Á. Linares-Solano, D. Cazorla-Amorós, Journal of Physical Chemistry C 112 (2008) 3827–3834.
[23] S. Domínguez-Domínguez, Á. Berenguer-Murcia, Á. Linares-Solano, D. Cazorla-Amorós, Journal of Catalysis 257 (2008) 87–95.
[24] I. Miguel-García, Á. Berenguer-Murcia, D. Cazorla-Amorós, Applied Catalysis B 98 (2010) 161–170.
[25] J.M. López, M.V. Navarro, T. García, R. Murillo, A.M. Mastral, F.J. Varela-Gandía, D. Lozano-Castelló, A. Bueno-López, D. Cazorla-Amorós, Microporous and Mesoporous Materials 130 (2010) 239–247.
[26] J.M. Campelo, F. Lafont, J.M. Marinas, Journal of Catalysis 156 (1995) 11–18.
[27] D. Lozano-Castelló, F. Suárez-García, D. Cazorla-Amorós, Á. Linares-Solano, in: F. Beguin, E. Frackowiak (Eds.), Carbon Materials for Electrochemical Energy Storage Systems, CRC, Press, Boca Raton (US), 2010, pp. 115–162.
[28] K.S.W. Sing, D.H. Everett, R.A.W. Haul, L. Moscou, R.A. Pierotti, J. Rouquerol, T. Siemieniewska, Pure and Applied Chemistry 57 (1985) 603–619.
[29] M. Boudart, Kinetics of Heterogeneous Catalytic Reactions, Princeton Univ. Press, Princeton, NJ, 1984.
[30] E. Ntainjua, A.F. Carley, S.H. Taylor, Catalysis Today 137 (2008) 362–366.
[31] Y. Borodko, S.E. Habas, M. Koebel, P. Yang, H. Frei, G.A. Somorjai, Journal of Physical Chemistry B 110 (2006) 23052–23059.
[32] Y. Borodko, S.M. Humphrey, T.D. Tilley, H. Frei, G.A. Somorjai, Journal of Physical Chemistry C 111 (2007) 6288–6295.
[33] J.K. Navin, M.E. Grass, G.A. Somorjai, A.L. Marsh, Analytical Chemistry 81 (2009) 6295–6299.
[34] J. Shie, C. Chang, J. Chen, W. Tsai, Y. Chen, C. Chiou, C. Chang, Applied Catalysis B 58 (2005) 289–297.
[35] J. Park, J. Lee, J. Miyawaki, W. Pang, S. Yoon, I. Mochida, Catalysis Communications 11 (2010) 1068–1071.